Chapter 5

Poly (Vinylidene Fluoride)/ Hydrated Antimony Pentoxide (HAP) Nanocomposite Films for the Application in High Energy Density Storage Supercapacitors

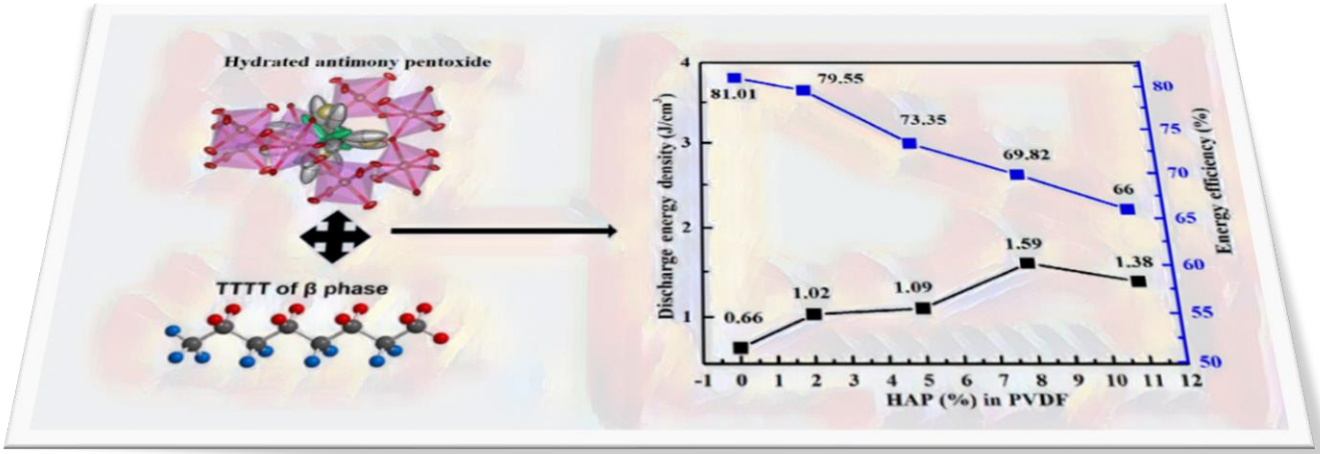

Chapter 5: Poly (vinylidene fluoride)/ hydrated antimony pentoxide (HAP) nanocomposite films for the application in high energy density storage supercapacitors

5.1 Introduction

The chapter 1 described the literatures of the nanocomposites with various types of fillers. The V_2O_5 and N-CDs have been used as filler in the chapter 3 and chapter 4 shows the better enhancement in the dielectric and storage properties. V_2O_5 have band gap around 2.3eV and N-CDs around 3 eV. Thus, the wideband gap semiconducting nanofillers could be useful as filler to reinforce in PVDF. So, we choose Sb_2O_3 having 3.2-3.7eV optical bandgap as filler [161]. The hydroxylation of the Sb_2O_3 is done to modify the surface to make better nanocomposite. The hydroxylation of the Sb_2O_3 resultant in formation of the hydrated antimony pentoxide (HAP), Previous reports tell that HAP is having proton conductivity [162].

In this chapter, we have synthesized the PVDF/HAP nanocomposite film using solution cast process, the volume percentage of the filler as 2vol%, 5vol%, 8vol% and 11vol% loaded in PVDF matrix to get better composition ratio for desired properties. To know the better formation of the better nanocomposite films, the morphological and structural analysis has been done. The improvement in the storage and dielectric properties has been studied with the help of various characterization techniques as discussed in the Chapter 2. The ferroelectric properties and dielectric properties have been discussed in detail. The energy density is calculated and breakdown strength was measured as capacitive devices for the all compositions.

5.2 Experimental

5.2.1 Synthesis of Hydrated antimony pentoxide (HAP)

The Sb_2O_3 purchased powder was further crushed to finer nano powder with the help of high energy ball mill (PM400MA, RETSCH, Gmbh, Germany) in ethanol medium. The nano powder was dried at 120℃. To get Hydrated antimony pentoxide ($(H_2O)_xH_{2-x}Sb_2O_6$), Hydroxylation of Sb_2O_3 was done with 30% H_2O_2 in water in a flask. The Sb_2O_3 nano powder was transferred to a flask containing the solution of 30% H_2O_2 in water and put at 105℃ for hydroxylation for 6 hours. The mixture was collected after drying at 120℃.

5.2.2 Synthesis of PVDF/HAP nanocomposite films

The synthesis of pure PVDF and Its nanocomposite films with HAP was done with the solution cast process. We have taken vol% of the filler to load in the polymer matrix. The HAP particles were poured in DMF and ultrasonicated for 1 hour and then stirred for 1 hour on the magnetic stirrer at 60℃ simultaneously the PVDF solution prepared with DMF solvent was also being stirred on another magnetic stirrer for 1 hour at the same temperature. The HAP was poured in PVDF solution and kept for further stirring on the magnetic stirrer at 60℃ for 8 hours. After completion of the stirring process, the mixture was ultrasonicated for 15 minutes followed by solution casting of slurry in the petre-dish and kept for drying at 120℃ for whole night to get self-standing nanocomposite film. The Figure 5.1 shows the whole synthesis process describe above. We have got the nanocomposite films with the thickness of 0.065±0.002 mm.

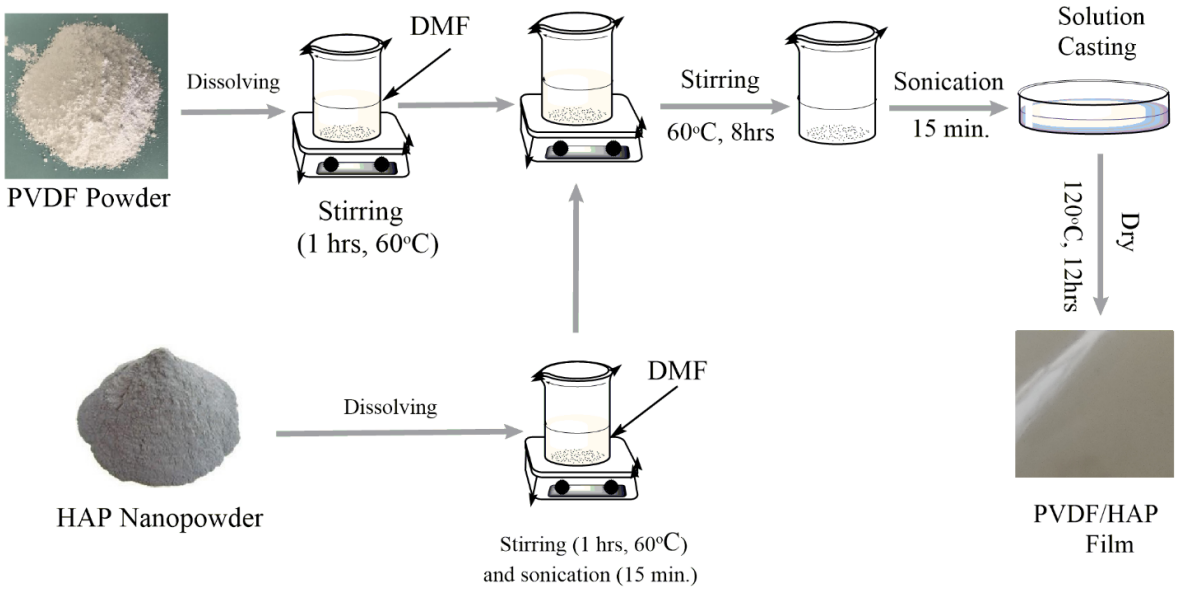

Figure 5.1 Schematic diagram of synthesis process of PVDF/HAP nanocomposite.

5.3 Results and Discussion

5.3.1 Characterization of filler Hydrated Antimony Pentoxide (HAP)

Analysis of the characterization of HAP nano powder is done in this section to know the formation of the HAP or the hydroxylation of the Sb_2O_3. The XRD pattern of the HAP is shown in the **Figure 5.2(a)** demonstrates the formation of the defect cubic pyrochlore structure belonging to the Fd3m (227) space group which has been confirmed with the help of X-pert High score software and matched with the previous reports as well [162,163]. According to the previous reports, the HAP has high proton conductivity as it has two H_3O^+ and H^+ which could act as a potential filler in the PVDF nanocomposite [162,163].

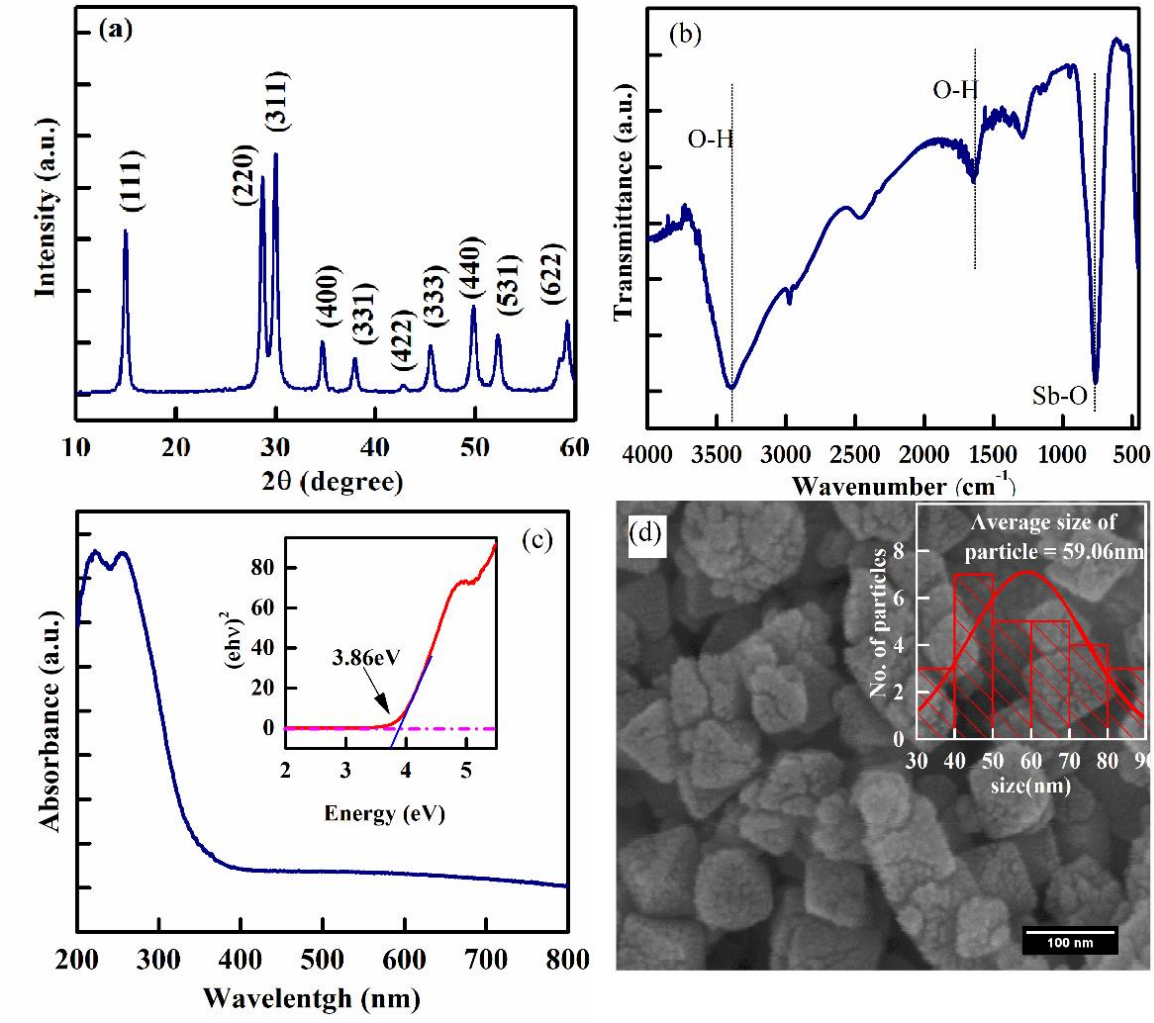

Figure 5.2 (a) X-Ray diffraction pattern, (b) FTIR spectra pattern (C) UV-Vis and Tauc's plot (inset), (d) HR-SEM image and histogram(inset), of HAP.

Figure 5.2(b) shows the FTIR spectra of Hydrated antimony pentoxide (HAP) nanoparticles which shows the hydroxylation of Sb_2O_3 nanoparticles by having -OH stretching and vibrating peaks at 3416 cm^{-1} and 1738 cm^{-1}. Sb-O-Sb vibration peak is present at the position of 733 cm^{-1} [162,164,165]. Sb_2O_3 is wideband gap semiconducting material, to confirm the bandgap of HAP, we performed the UV-Vis. spectrum measurement, with the help of Tauc's plot, the calculated bandgap is around 3.86 eV as can be seen in **Figure 5.2(c)**. The FESEM image of HAP nano powder revealed the size of the nanoparticles as shown in the **Figure 5.2(d)**, in the inset, it can be seen that the average size of nanoparticle is around 59.06 nm.

5.3.2 Structural analysis of PVDF/HAP nanocomposite films

XRD, FTIR and DSC Analysis was done to investigate the electroactive phase formation in the nanocomposite films. XRD patterns for all the composition are shown in the Figure 5.3(a), the XRD pattern of Hydrated antimony pentoxide (HAP) has already been discussed in the section 5.3.1. The XRD pattern for the pure PVDF and Nanocomposite shows the formation of crystalline phases or electroactive phase (β, γ-phase) with α-phase as non-electroactive phase. The peaks of the α-phase can be observed at 18.4º, 26.5º, 47.3º. The significant peaks at the 26.6º, 36.1º, 42.3º are assigned to the β-phase. the peaks at the 18.5º, 20.3º and 39.4º are related to the electroactive γ-phase having mixed trans and gauche conformation [166–170]. Due to presence of the HAP in the PVDF matrix, the intensity of peaks related to PVDF is lower as compare to the peak related to the HAP but overall crystallinity of nanocomposite film is increased due to the increment of filler loading from 2vol% to 11vol%. The structure investigation is also done with the help of FTIR spectra as shown in the Figure 5.3(b) to better understanding of the presence of the different phase in the nanocomposite films with the varying filler loading vol%. The α, β and γ-phase in the PVDF and its nanocomposites are stable phases, getting these phases generally facile. The formation or achieving δ-phase is difficult as it is less table compare to the α, β and γ-phase. The characteristic peaks of the non-electroactive phase (α-phase) are assigned to the 532 cm^{-1}, 614 cm^{-1}, 764 cm^{-1}, 1423 cm^{-1} position in the FTIR spectra. The electroactive phases β, γ-phases are assigned to 510 cm^{-1}, 832 cm^{-1}, 1071 cm^{-1} and 1275 cm^{-1} and 482 cm^{-1} , 811 cm^{-1}, 832 cm^{-1}, 881 cm^{-1} , 1234 cm^{-1} respectively. The most significant peaks for the electroactive phases (β, γ-phases) are 832 cm^{-1}, 1234 cm^{-1}, 1275 cm^{-1} [148,166–171]. The α-phase has significant peak at 764 cm^{-1} [148,166–171]. The broad peak at 733 cm^{-1} is related to the Sb-O-Sb vibration of the HAP loaded in the PVDF matrix. Sb-O-Sb is becoming dominant peak with the increasing of filler loading in the PVDF,

at 11 vol% of the HAP, the same peaks is broad which may have some adverse effect on the electroactive formation of PVDF.

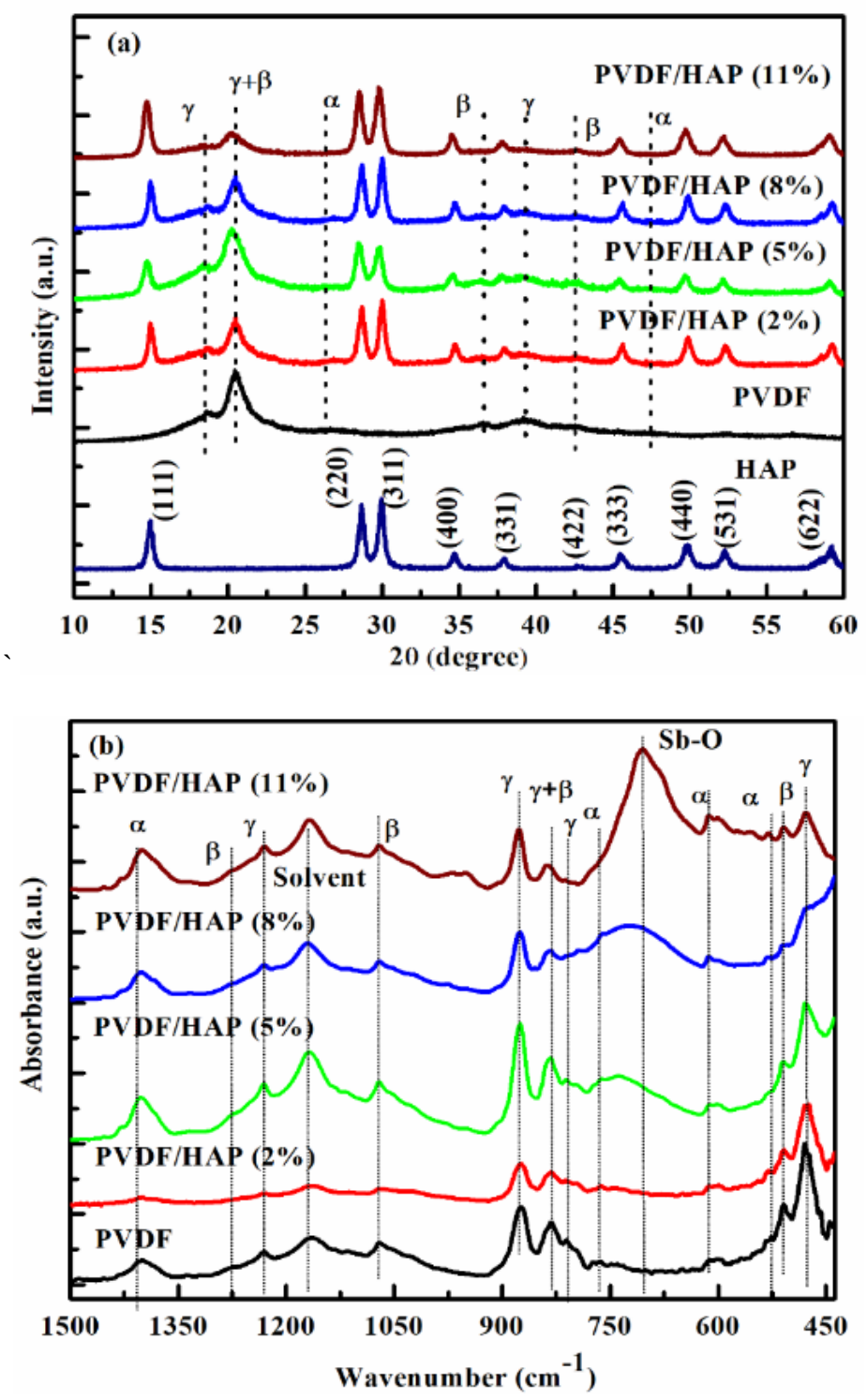

Figure 5.3(a) X-Ray diffraction pattern, (b) FTIR Spectra of pure, PVDF and PVDF/HAP nanocomposite films.

The DSC measurement was done to study thermal stability and crystalline nature of nanocomposite films. In the Figure 5.4, in pure PVDF, there are two endothermic melting peaks at 161.6℃ and 167.0℃ which are referred to premature α-phase and α, β, γ-phase respectively[97,148,168]. It's not easy to distinguish the peaks for the particular phase melting but shifting this peak toward higher temperature is the evidence of the presence of the electroactive phase. In nanocomposite films, the endothermic peak related to electroactive phase shifts toward higher temperature due to the coherence energy for the electroactive phases is higher than the non-electroactive phase. The coherence energy depends on the dipolar interaction inside the nanocomposite films [97,132,148,168,172–174].

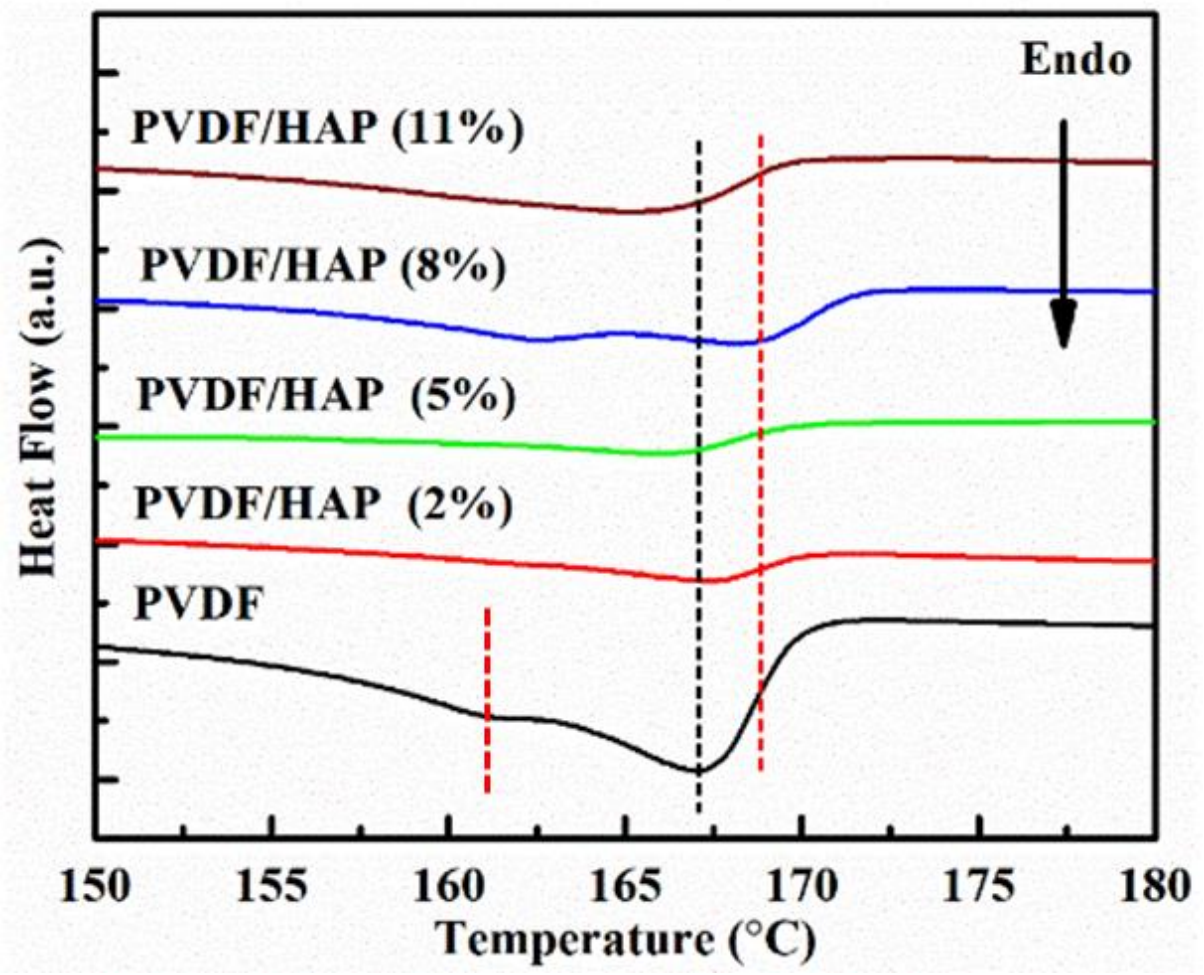

Figure 5.4. DSC analysis of pure PVDF and PVDF/HAP nanocomposite films.

5.3.3 X-ray photoelectron spectroscopy (XPS) analysis

Study of surface chemistry of the PVDF and PVDF/HAP (8%) was done with the XPS as shown in the Figure 5.4. There, we can see a minor difference between the peak position in XPS survey of pure PVDF and PVDF/HAP film in the range around 528 to 544 eV as shown Figure 5.4(a). The PVDF/HAP nanocomposite has the peaks for Sb $3d_{5/2}$ and Sb $3d_{3/2}$ located at 530.2 and 539.6eV, respectively evidencing the presence of the HAP in the PVDF matrix. In addition to this, the Sb $3d_{3/2}$ peak displays good symmetry; consequently, the peak can only be assigned to the Sb^{5+} that conclude that the Sb_2O_3 is transformed to HAP and present in this form inside the PVDF matrix. There is an overlap at 530 eV between the peaks of Sb $3d_{5/2}$ and O 1s, and we deconvolve this peak using the double-peak property of the Sb 3d orbital. As a result, the binding energy of the lattice oxygen corresponds to 530.04, 531.31, and 532.41 eV, which are corresponding to the adsorbed oxygen, surface hydroxyl oxygen, and lattice oxygen, respectively.

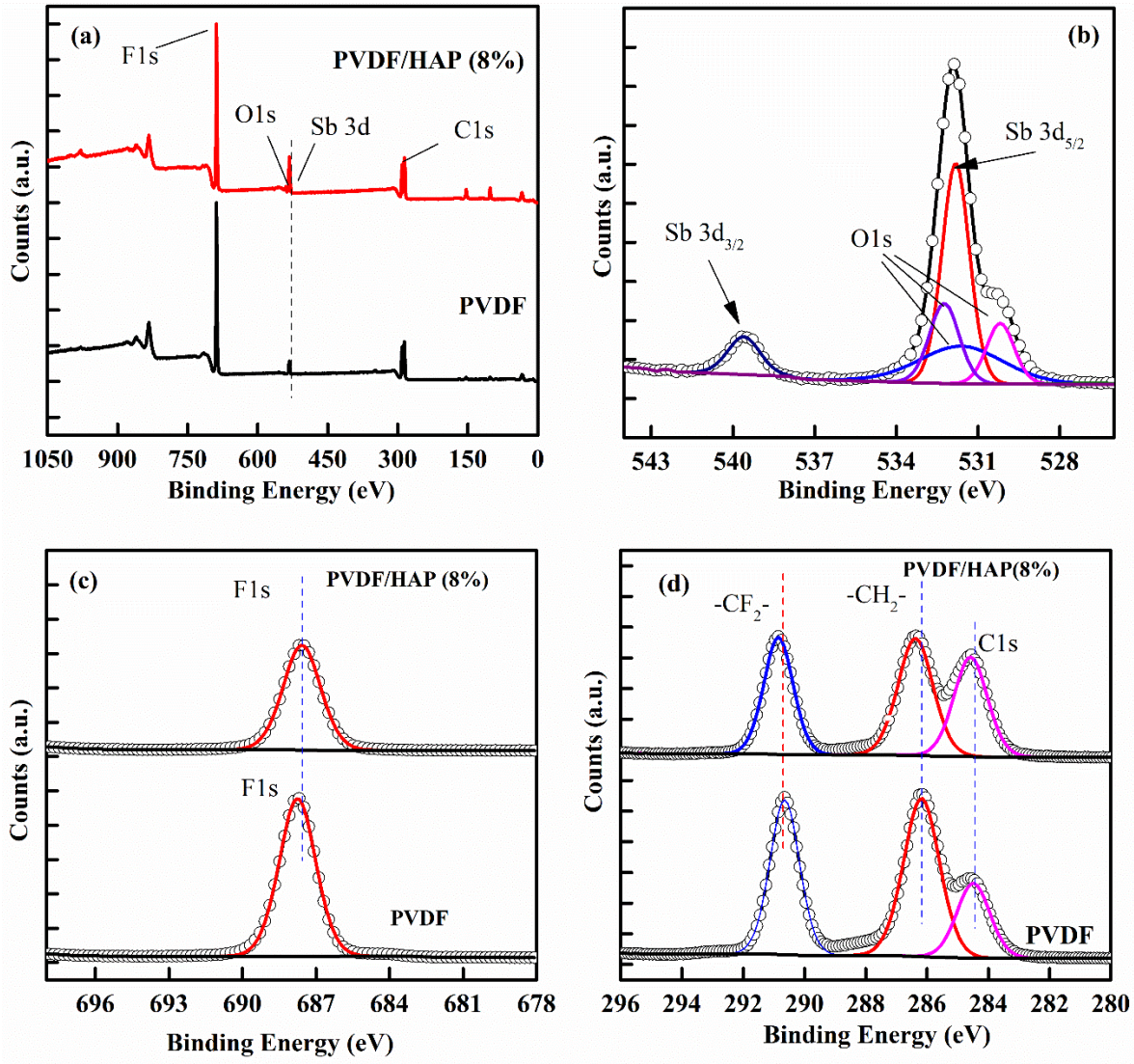

Figure 5.5 (a) XPS survey of the PVDH/HAP (8%), Zooming out the peak of (b) Sb, (c) F1s (d) C1s.

The F1s peak position (687.60 eV) of the PVDF/HAP has recorded minor shift from the F1s peak of the pure PVDF (687.75 eV). The deviation can be ascribed to the intermolecular interaction to the highly polarized backbone's ($–H^{\delta+}–C^{\delta+}–F^{\delta–}–$ dipoles) hydrogen atom of PVDF and -OH of the HAP [104,149]. The zoom-in of the C1s peak position in PVDF and PVDF/HAP shows that C1s spectrum is showing three peaks corresponding to $–CH_2$ and $–CF_2$ of the PVDF backbone at the position 290.9 eV and 286.6 eV respectively, the third shoulder peak is related to the non-oxygenated carbon ($-C_xH_y-$) at the position 284.6 eV. In PVDF/HAP, the C1s corresponding to $–CH_2$ and $–CF_2$ are shifted to the higher binding

energy caused by the presence of oxygenated carbon. The presence of the oxygenated carbon in the PNC film proves the inclusion of the HAP [149].

5.3.4 Morphological analysis of PVDF/HAP nanocomposite films

To know the surface morphology of the nanocomposite films, the images given in the Figure 5.5 are analyzed. The surface of the pure PVDF is full of spherulites. The size of the spherulite in pure PVDF is around 11μm. As the filler is loaded with 2 vol%, the decrement in the size of the spherulite is not observable but as the amount of filler loading is increased further to 5vol% and 8vol % then the size of the spherulites decrease with more numbers of the spherulites as shown in **Figure 5.6 (c, d)**. In **Figure 5.6 (d)** it can be observed as the loading of filler is increased then the porosity in the film is decreased and film seems to be smoother. At 11 vol% loading, the spherulites almost are not observable and film is smooth with no porosity. Crystallization is a gradual process that involves the formation of nuclei and the growth of crystals[111,152,175]. As the filler being loaded to the matrix, the average spherulite size shrank but the more numbers of spherulites are there. The nanofillers act as nucleating sites, allowing nucleation to occur at a faster rate than grain growth that leads to smaller spherulites due to higher number of spherulites available[111,152,175]. A smooth surface could come from the densification and orderly arrangement of crystalline grain arrays[111,152,175]. The **Figure 5.6(f)** shows the elemental mapping showing the presence of all elements with particular color.

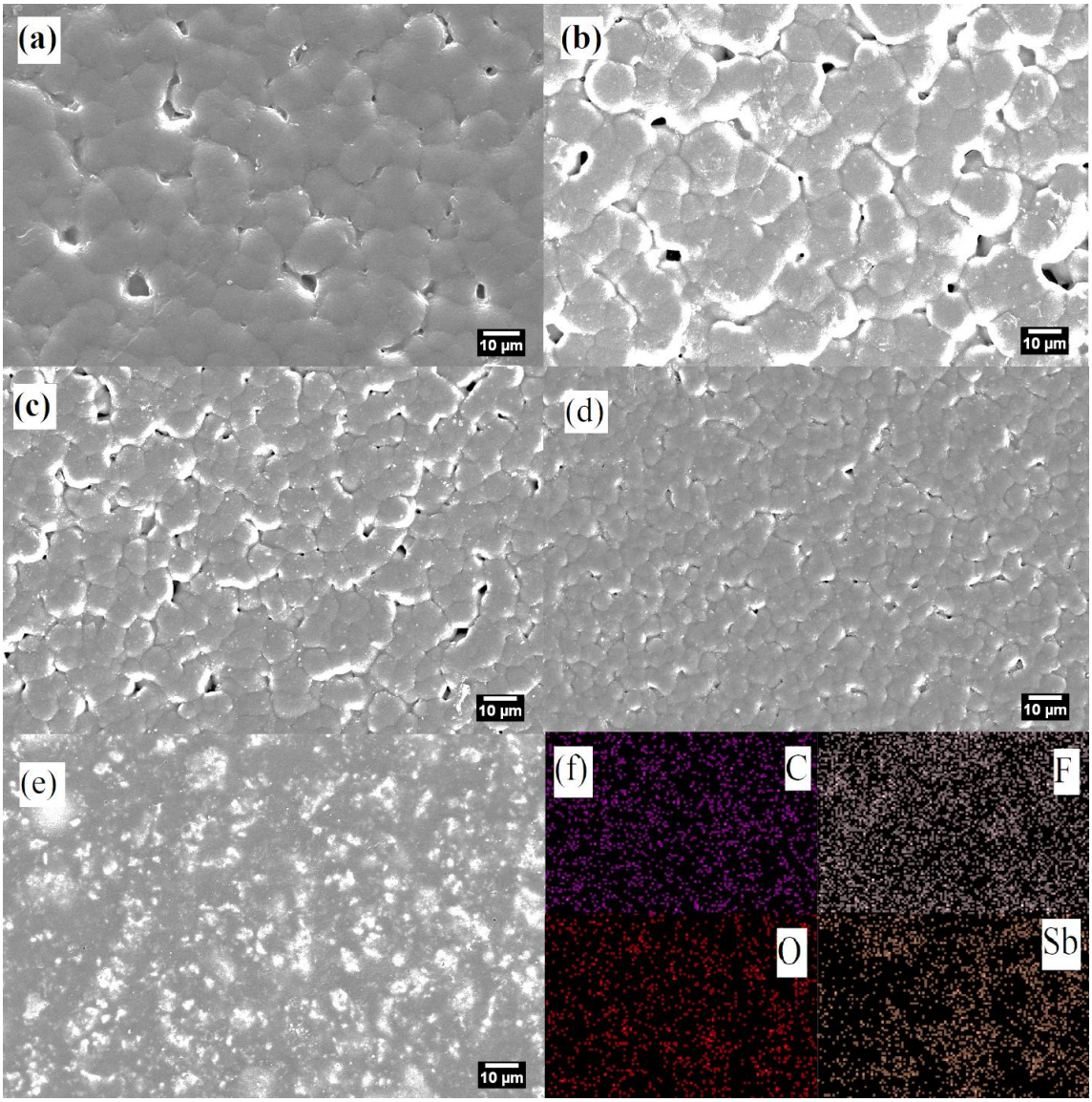

Figure 5.6 FESEM image of (a) pure PVDF Film, (b) PVDF/HAP (2%), (c) PVDF/ HAP (5%), (d) PVDF/ HAP (8%), (e) PVDF/ HAP (11%) and (f) Elemental mapping images of PVDF/ HAP (8%) with elements.

5.3.5 Dielectric and ferroelectric properties of PVDF/ HAP nanocomposite films

The dielectric properties of the nanocomposite films are shown in the **Figure 5.7**. As we already know the thermal stability of PVDF and its nanocomposite, the dielectric constant and loss is measured from room temperature to 120°C and plotted for the 1kHz in **Figure 5.7(a, b)**. In **Figure 5.7(c, d)**, the dielectric constant and loss vs frequency is shown. The dielectric constant of PVDF is ~9. The loaded filler HAP in the nanocomposite matrix has increased the

dielectric constant to ~28 that is more than 3 times as shown in the **Figure 5.7(a, c)** for the 8 Vol%. Even with 2 vol% filler the dielectric constant increased to 14 but at 11 vol% of filler loading the dielectric constant increased but less than the increment with 5 vol% loading. The increment in the dielectric constant is mainly due to the interfacial polarization [174,176,177]. This interaction can be defined by Maxwell Wagner Sillar (MWS) interfacial polarization[174,176,177]. The effect of the MWS interface polarization can be justified as the frequency is increasing, the dielectric constant is also decreasing as shown in the **Figure 5.7(c)**. This is due to the reason that the speed of dipole relaxation of space charge and dipolar polarization could not keep up with the variation in the electric field, resulting in a decrement in the dielectric constant with increasing frequency. The dielectric loss is determined by the material's conduction loss and dielectric polarization loss, which is primarily caused by space charge migration and molecular dipole movements[174,176–179]. As the frequency increases, the intensity of the space charge increases, resulting in an increase in dielectric loss, as seen in the range 10^3 to 10^6 Hz in **Figure 5.7(d)**. The dielectric loss has not increased much for the 2 Vol% to 8 vol% but for the 11 vol% it has increased to some extent that's because, the HAP has proton conductivity and till 8 vol% the proton was absorbed by the negative charge present in the PVDF but as the concentration is increased further more number of protons are there so the loss has increased. This could be described with the help of percolation threshold. The percolation phenomenon is a critical characteristic for investigating the dielectric properties of PVDF based nanocomposites. When the volume proportion of conductive filler reaches a critical amount, the composites conductivity and permittivity increase by several orders of magnitude (percolation threshold).

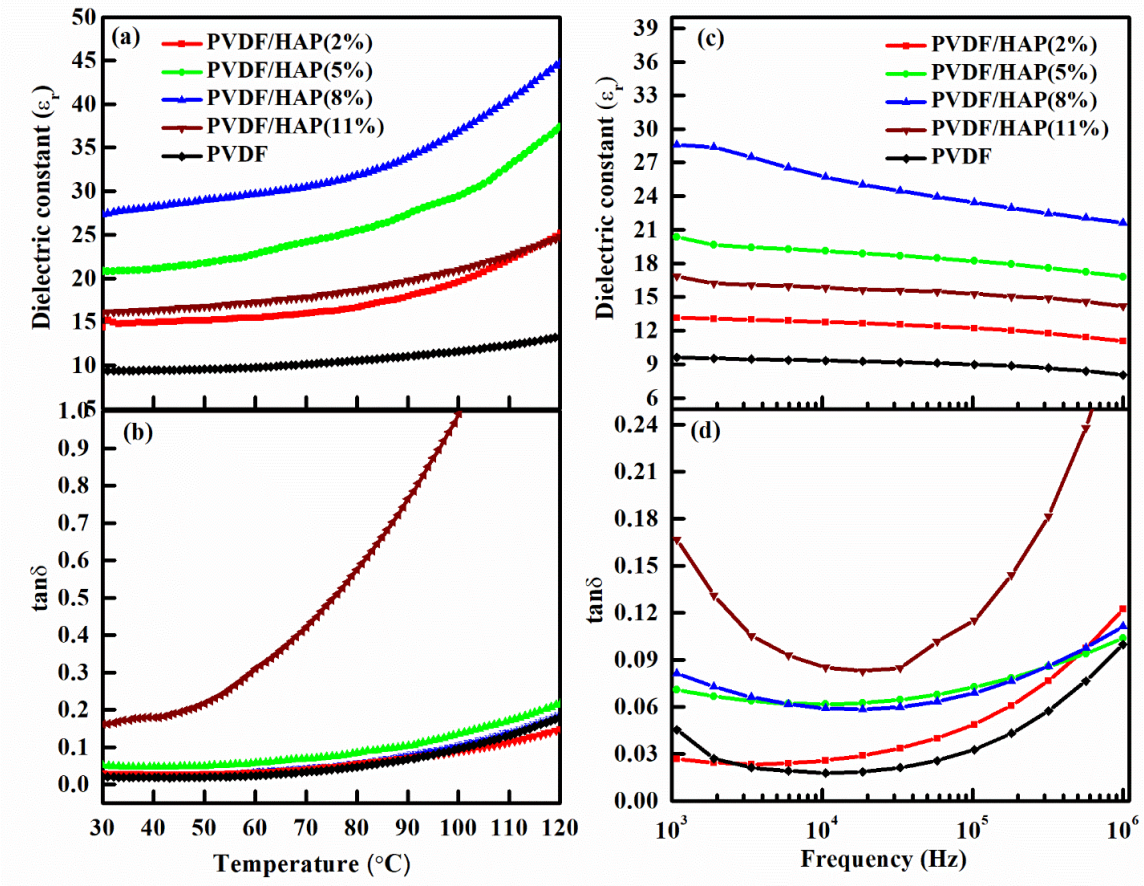

Figure 5.7(a) Dielectric constant vs temperature, (b) Dielectric loss vs temperature, (c) Dielectric constant vs frequency and (d) Dielectric loss vs frequency, of all compositions.

The proton conductivity contribution at 11 vol% filler loading can be seen in the Figure 5.8. The conductivity is calculated with the help of expression $\sigma = 2\pi f\ \varepsilon_0\ \varepsilon_r\ \tan\delta$, where σ is conductivity, 'f' is frequency and ε_0 is the permittivity of space. As the frequency is increasing the conductivity is also increasing. This can be assumed that with increasing frequency, the dipoles are not that quick to align with the electric field due to high frequency, thus the conduction mechanism is playing role to enhance the conductivity.

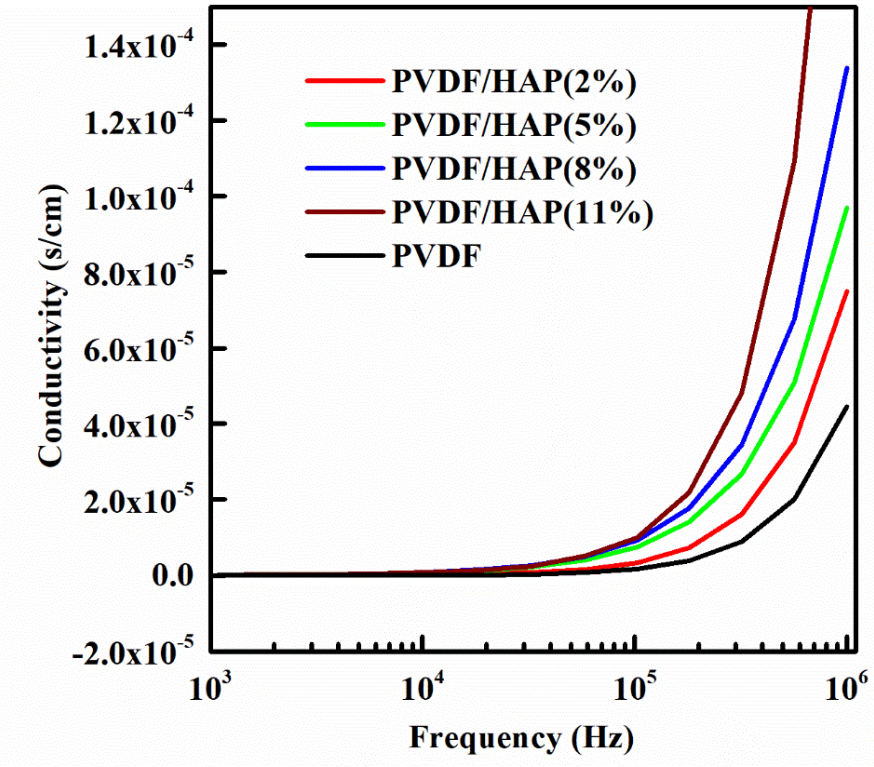

Figure 5.8. The AC conductivity of the pure PVDF and nanocomposite films.

The Polarization vs Electrical field (P-E Loop) measurement is done to analyze the ferroelectric properties of the pure PVDF and its nanocomposite with HAP as show in the **Figure 5.9**. The influence of charge generation inside nanocomposite films may be studied using the P-E Hysteresis loop. The P-E loop measurement was done at room temperature for the all the nanocomposite and pure PVDF films. The effect of the HAP filler on the P-E loop can be clearly seen with the increasing loading vol %. The value of the Pr (remanent polarization) and P_m (Maximum polarization) for the pure PVDF and nanocomposite films are shown in the table given below. The highest value of the polarization is for the 8 vol% loading in PVDF that is 2.63 µC/cm^2 as compared to pure PVDF with 1.08 µC/cm^2 due to the interfacial polarization[174,176–179]. The HAP has proton conductivity and is able to trap the charge from PVDF matrix to create dipoles. As the filler loading increased to 11 vol %, the value of the polarization decreases and loop is more lossy compared to the 8 vol% loaded films that's

because as the HAP have proton in more numbers which are responsible for the lossy nature and decreased number of dipoles so the polarization.

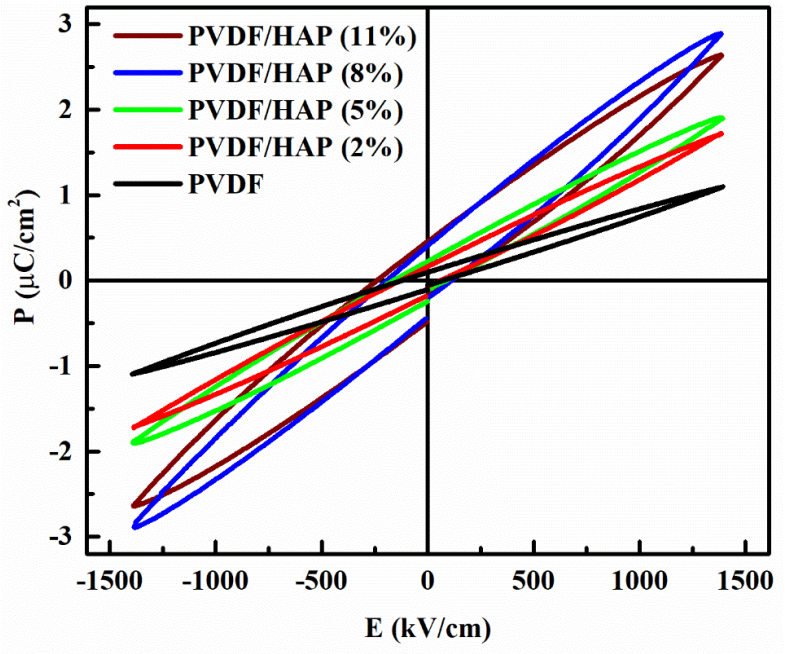

Figure 5.9. P-E hysteresis loop of all compositions

Table 5.1 The P_{max} and P_r of the all nanocomposites and pure PVDF.

Sample	P_r (μC/cm²)	P_{max} (μC/cm²)
Pure PVDF	0.10	1.08
PVDF/HAP (2%)	0.15	1.72
PVDF/HAP (5%)	0.22	1.90
PVDF/HAP (8%)	0.46	2.88
PVDF/HAP (11%)	0.40	2.63

5.3.6 Breakdown strength, Energy density and Energy discharge efficiency of PVDF/HAP nanocomposite films

As we know the energy density depends on the breakdown strength. So, the study of dielectric behaviour should be done. The breakdown strength of the PVDF and nanocomposite films was calculated with the help of an AC electrical breakdown strength test setup. **Figure 5.10** shows the breakdown strength calculation with the help of Weibull distribution function equation (1.17) as $P(E) = 1- \exp (- (E_i / E_b)^{\beta})$, where $P(E) = i /(n+1)$ is the cumulative probability of failure, E_i is the experimentally measured value of electric field at which sample breakdown, β is the shape parameter related to linear fit. The larger the β means the composite has less defects and more uniform vice versa[134,174,180]. We draw a plot between the two parameters X_i, Y_i which are given by the equations given below as equation (1.18) and (1.19).

$$X_i = \ln (E_i)$$

$$Y_i = \ln \left[-\ln \left(1 - \frac{i}{n+1}\right)\right]$$

Where, i is the consecutive number of samples in n numbers of samples.

With the varying vol % of the filler in PVDF matrix show the variation in the breakdown strength, the breakdown strength decreases as the filler loading is increasing due to the presence of conducting protons in the filler which helps in making path for charge to pass through the polymer matrix and that leads to breakdown of the nanocomposite film. The poor interfacial compatibility between the organic and inorganic phases may also be another reason for the early breakdown, agglomeration of the filler also increases the chances of the breakdown at the lower field[134,174,180]. Though the porosity in the film is not increased as we can observe in FE-SEM images, the films have become smoother so the β value is higher for the films. It can be clearly seen in the **Figure 5.10** that as the vol % is at 8 till then the breakdown strength does not decrease sharply but as the vol % increased to 11, the breakdown decreases sharply due to

presence of more conducting paths due to higher proton density inside the film due to the filler HAP. So, the loading of filler more than 8 vol % would not be advantagoues.

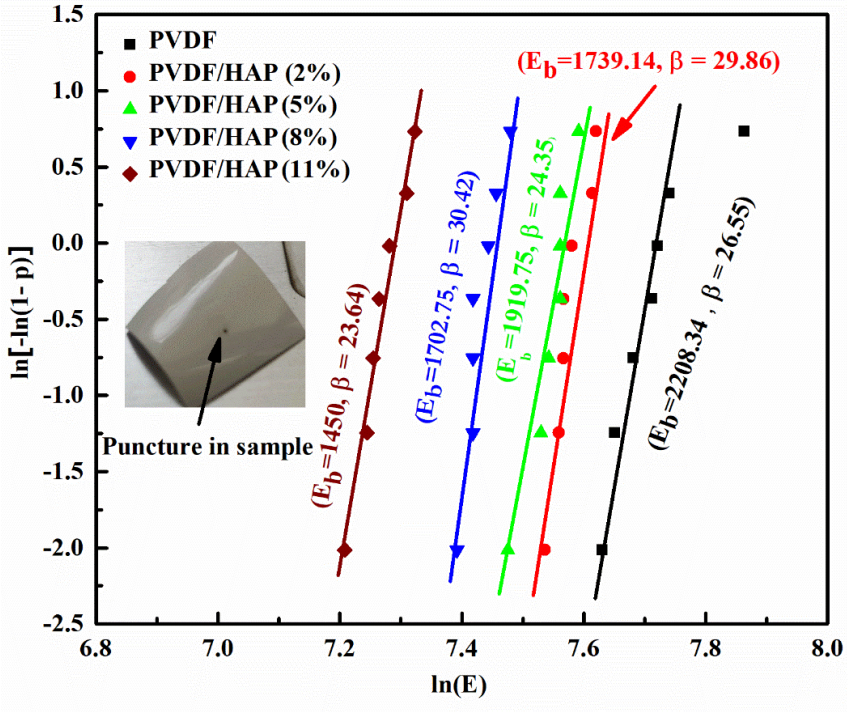

Figure 5.10. Weibull distribution of all composition.

The discharged energy density of the PVDF/HAP nanocomposite films are calculated from the P-E loop using the equations (1.10) and (1.11) as given below[181].

$$\text{Total energy density } (U_c) = \int_0^{P_{max}} E\,dp$$

$$\text{Discharge energy density } (U_d) = \int_{P_r}^{P_{max}} E\,dp$$

The calculated energy density for all samples is at 1400 kV/cm^2 electric field as shown the **Figure 5.12.** The discharge energy density at 1400kV/cm^2 of the PVDF is 0.66J/cm^3. The loading of the filler in the PVDF matrix enhanced in the energy density almost more than 2 times at the applied 1400kV/cm^2 field. For the 8 vol%, The energy density is 1.59 J/cm^3 and as the filler loading is 11 vol %, the energy density decreases due to the less polarization and higher loss.

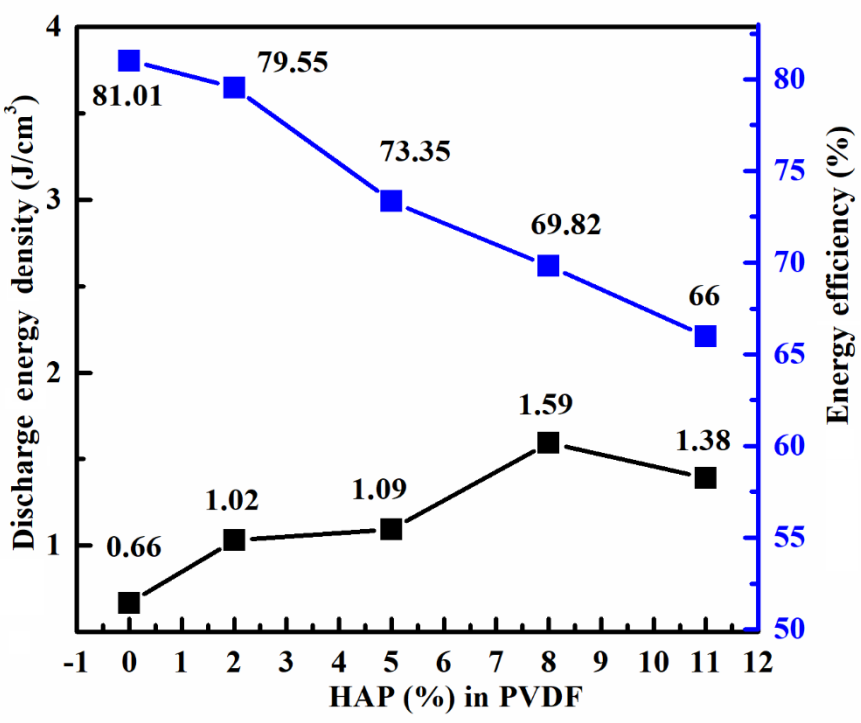

Figure 5.12 Discharged energy density and discharge energy efficiency of PVDF, PVDF/HAP nanocomposites as function of applied field at 1400kV/cm.

In Figure.12, the energy discharge efficiency is calculate using the equation (1.13) as given below[14]

$$\text{Discharge energy efficiency } (\eta\%) = \frac{U_d}{U_d+U_l} \text{ x } 100$$

where U_d and U_l are discharge energy density and energy loss density respectively. The calculate efficiency is 69.82% as shown in the **Figure 5.12**. The final results show the improvements in dielectric properties and energy density also increased. We can say that HAP as a filler can be good option to enhance the properties of PDVF and the enhancement in the energy density of nanocomposite film is useful to use in energy storage applications.

5.4 Conclusion

The synthesis of the filler HAP is done with the facile process using the nano powder Sb_2O_3 followed by hydroxylation with H_2O_2. The phase identification of the HAP formation is done

with the help of XRD, FTIR, it is confirmed that it has pyrochlore cubic structure belonging to the Fd3m (227) space group. The facile solution cast synthesis process of nanocomposite films with variation of the volume % of the filler in the PVDF matrix is shown in this work. The self-standing flexible PVDF/HAP nanocomposite films are characterized with help of XRD, FTIR and SEM to know the electroactive phase to confirm the presence of the ferroelectricity and morphology of nanocomposite films. The ferroelectric nature of the films was studied with the help of PE loops. The dielectric constant was recorded to understand the capacitive behaviour of the films. With 8 vol% filler loading in the PVDF matrix, the dielectric constant is achieved to 28.08, P_{max} is 2.88($\mu C/cm^2$) and Energy density is 1.59 J/cm^3 at 1400kV/cm electric field. The enhancements in the nanocomposite films storage and dielectric properties are significant as compare to the pure PVDF. These films can be used as capacitive energy storage device.